ORIGINAL ARTICLE

Experimental investigation on tool wear in ultrasonic vibration-assisted turning of SiCf/SiC ceramic matrix composite

Cong Liu[1,2] · Wenhu Wang[1,2] · Yifeng Xiong[1,2] · Bo Huang[1,2] · Liangwan Li[1,2]

Abstract

Silicon carbide fiber-reinforced silicon carbide matrix composites have attracted attention due to superior properties, such as low density, high strength, and high-temperature resistance. However, it often faces severe tool wear during cutting, with the fibers and matrix material being of high hardness and brittleness, which has an inevitable effect on the engineering application of this kind of material. In this paper, wear volume V_W is used to evaluate the tool wear through solid modeling and parameter measurement based on the tool wear topography in turning of SiCf/SiC ceramic matrix composites. Conventional turning (CT), ultrasonic vibration-assisted turning (UVAT), and ultrasonic vibration-assisted turning with water cooling (W-UVAT) experiments are carried out using CBN, PCD, and PDC tools to investigate and analyze the cutting performance. In the meantime, the tool wear mechanism and form are studied based on the analysis of ultrasonic vibration on tool wear, the geometric position of wear, accumulation of cutting workpiece powders, and tool wear curve. Experimental results found that the PDC tool obtains the best cutting performance, which is more suitable for turning silicon carbide fiber-reinforced silicon carbide matrix composites. Within the experimental parameters, with the increased ultrasonic amplitude A, V_W decreases first and then increases, reaching a minimum at A which is 3 μm. The main wear mechanism of the PDC tool is abrasive wear, and the primary wear form is the spalling of polycrystalline diamond abrasive grains.

Keywords SiCf/SiC · Turning · Ultrasonic vibration · Wear volume · Cutting performance · Mechanism

1 Introduction

Fiber-reinforced ceramic matrix composites (FRCMC) have attracted attention for high specific strength and high-temperature resistance, such as C/C composites, Cf/SiC ceramic matrix composites, and SiCf/SiC ceramic matrix composites [1, 2]. It has become a strategic structural material for higher strength and higher temperature materials and has broad applications in aerospace, military, and other fields [3, 4]. FRCMC are typically hard, brittle, and difficult-to-cut materials, but it is difficult to obtain satisfactory machining characteristics with traditional machining methods. Ultrasonic vibration-assisted machining technique is an advanced machining method for difficult-to-cut materials. Many researchers have shown that the application of ultrasonic vibration in conventional cutting is beneficial to improve the processing characteristics (surface roughness, cutting force, cutting heat, tool wear, etc.) [5–9]. However, there are still problems with the machining application of FRCMC, such as feasible machining methods, cutting tool selection, and severe tool wear, and so on.

With the existence of hard matrix and reinforced fibers, FRCMC are easy to cause severe tool wear during processing, which has a significant influence on the quality of the workpiece and processing efficiency. Tool wear has always been studied as an extremely important factor. Establishing a unified evaluation system is a significant task in studying the wear resistance with different cutting tools. The International Organization for Standardization stipulates flank wear width VB as the tool wear standard (ISO 3685:1993).

✉ Yifeng Xiong
  xiongyf@nwpu.edu.cn

1 Key Laboratory of High Performance Manufacturing for Aero Engine, Ministry of Industry and Information Technology, School of Mechanical Engineering, Northwestern Polytechnical University, Xi'an 710072, Shaanxi, People's Republic of China

2 Engineering Research Center of Advanced Manufacturing Technology for Aero Engine, Ministry of Education, School of Mechanical Engineering, Northwestern Polytechnical University, Xi'an 710072, Shaanxi, People's Republic of China

Prasad et al. [10] used the flank wear height as the evaluation parameter and studied the relationship between the amplitude and tool wear by finite element simulation and experiments. Shen et al. [11] evaluated the wear of the diamond grinding wheel in the process of ceramic materials using the protruding height of the diamond abrasive grains and the radial wear value and found that ultrasonic vibrations could maintain a stable sharpness on the working surface of the grinding wheel. Palanikumar et al. [12], Das et al. [13], and Airao et al. [14] also adopted *VB* as the evaluation parameter for tool wear. Based on three types of tool-workpiece separation criteria, Feng et al. [15] proposed a tool wear (*VB*) rate predictive model, applicable for vibration in three directions. In addition, based on the sensitivity analysis, they found that a smaller axial depth of milling, larger feed per tooth, or higher cutting speed will result in a higher flank wear rate. And the effect of vibration parameters is less significant. However, the wear behavior of the tool is a change in the volume of space, and there is a certain extent of wear in both axial and radial directions for the worn tool. The same *VB* may represent different wear volumes. *VB* may be more suitable for qualitative comparative analysis of the tool wear during machining. Therefore, Liu et al. [16] established a geometric model of the tool wear volume and calculated the tool wear volume using the calculus method. Ma et al. [17] established a mathematical model of the tool wear volume with geometry and kinematics analysis for brittle materials and studied the influences of cutting speed, cutting depth, and feed rate on the tool wear.

Basically, with the immature preparation process of SiC_f/SiC ceramic matrix composites, the workpieces are plate-shaped, which focus on milling, grinding, and drilling. At present, there are few published researches on cylindrical or rod-shaped SiC_f/SiC ceramic matrix composites. The choice of cutting tool has a serious impact on tool wear, tool life, and the quality of the finished product. Many experimental investigations have been conducted on hard and brittle materials. Zhao et al. [18] used a diamond tool to cut glass SF6 in ductile mode, showing that applying ultrasonic vibration to the tool is beneficial to increase tool life and improve surface finish. In the study of Sarma et al. [19], they found that using air cooling could significantly reduce the wear and cutting force of ceramic tools during high-speed cutting of gray cast iron and provide a better surface finish. Dai et al. [20] showed that the surface roughness could be less than 0.025 μm by ultrasonic face grinding of SiC ceramic with the designed diamond electroplated wheel under the condition of high wheel speed and minor vibration amplitude closing to 0.2 μm. Meanwhile, in the face of CFRP and FRCMC with higher hardness, researchers have also conducted a great number of studies on the tool performance. Rajasekaran et al. [21] obtained suitable parameters for machining CFRP with ceramic tools and obtained the satisfied surface roughness by orthogonal experiments and variance analysis. Shan et al. [22] conducted orthogonal tests of C/C composites with cemented carbide milling cutters and verified the reliability of the predictive model of the cutting force. Babbar et al. [23] found applying ultrasonic vibration could reduce tool wear by milling tests of C/SiC ceramic matrix composites with diamond abrasive tools. Zhang et al. [24] indicated that PCD tools had better tool life and cutting performance when milling SiC_f/SiC ceramic matrix composites using PCD and CVD diamond tools. In the meantime, Dhokey et al. [25] showed that diamond tools have good wear resistance. However, for the higher hardness of SiC_f/SiC ceramic matrix composites, there is a lack of turning research results for this material. The applicability of existing tools still needs to be investigated and analyzed.

The investigation on tool wear mechanism could help to reduce wear and improve machining quality. Through MMC material turning experiments, Kılıçkap et al. [26] found that the built-up edge micro-cut the workpiece and reduced tool wear. It showed that the tool wear mechanism was abrasive, and there was no sign of chemical wear. Bhushan et al. [27] showed that the tool wear mechanism of turning AA7075/SiC composites was mainly two-body and three-body wear. Wu et al. [28] and Li et al. [29] also came to the same conclusion. Quan et al. [30] showed that the main wear mechanism of conventional tools cutting SiC particle-reinforced aluminum matrix composites was abrasive wear. For high-hardness tools, the main damage mechanism during cutting was a brittle fracture. Zeng et al. [31] found that there were two stages of tool wear when processing SiC with diamond tools. The first stage was mainly wear, and the second stage was mainly fracture. Liu et al. [32] used diamond tools to mill C/SiC composites by ultrasonic vibration-assisted and conventional milling. It showed that the main wear mechanism of the tool flank was abrasive wear, and the main wear form was coating peeling.

The traditional tool wear evaluation method is the flank wear width *VB*, which has some certain limitations and does not reflect the essence of tool material removal. At present, there are few studies on the tool wear volume. The lack of SiC_f/SiC ceramic matrix composites has resulted in few published research reports on turning. The hardness of the materials that have been published for turning research is far smaller than this material, and the applicability of the existing tools needs to be further studied. In addition, there are relatively few studies on the tool wear mechanism in the cutting of SiC_f/SiC ceramic matrix composites.

Hence, in this paper, to investigate the turning problem and tool wear in machining SiC_f/SiC ceramic matrix composites, conventional turning (CT), ultrasonic vibration-assisted turning (UVAT), and ultrasonic vibration-assisted turning with water cooling (W-UVAT) experiments were carried out. Through the wear topography, solid modeling,
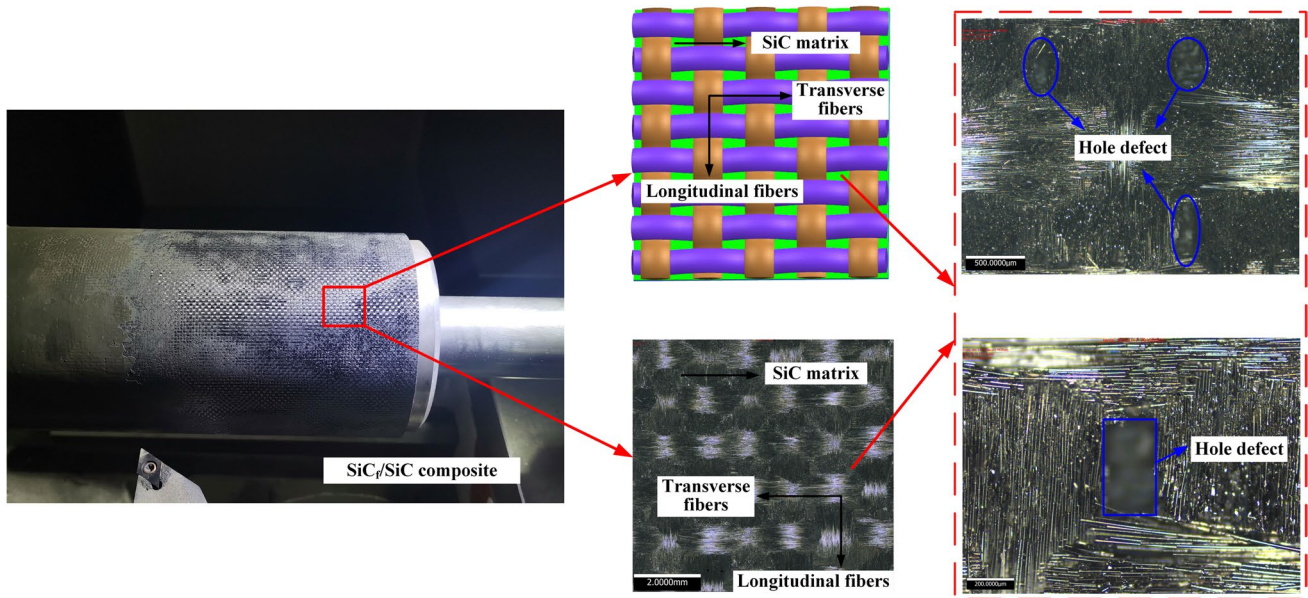
Fig. 1 SiC$_f$/SiC ceramic matrix composites

and measurement of wear parameters, tool wear volume V_W was calculated. The turned surface roughness, tool wear, and cutting force were selected for describing and analyzing the cutting performance. The influence of ultrasonic amplitude on tool wear was also studied. Eventually, based on the analysis of the geometric position of wear, accumulation of cutting workpiece powders, and tool wear curve, the tool wear mechanism and form were investigated and analyzed.

2 Material and experimental methods

2.1 Material and tool

In this study, the workpiece materials are cylindrical SiC$_f$/SiC ceramic matrix composites, which consist of SiC fibers and SiC matrix, and the workpiece surface is an orthogonally woven structure, as shown in Fig. 1. SiC$_f$/SiC ceramic matrix composites have a certain porosity with the woven structure and the preparation process of the material, resulting in many original hole defects on the surface and inside of the material, as seen on the right of Fig. 1. And the original hole defects are mainly formed at the junction of warp and weft. In the preparation process, the deposition of SiC matrix material is incomplete, resulting in less infiltration of the matrix below the surface. The hole defects in the weaving process cannot be filled and are gradually exposed with machining.

The mechanical properties of SiC$_f$/SiC ceramic matrix composites are shown in Table 1. The size of the workpiece is $\Phi 100 \times 200$ mm, and the wall thickness is 5.5 mm. Due

Table 1 Mechanical properties of SiC$_f$/SiC ceramic matrix composites

| Material properties	Value
Density (g/cm^3)	2.52
Porosity (%)	10
Radial tensile strength (MPa)	288.78
Interlaminar shear strength (MPa)	45.29
Room temperature compressive strength (MPa)	544.63
Room temperature fracture toughness (MPa)	26.53

Table 2 Geometric parameters of the turning tool

Tool nose angle	Tool nose radius	Rake angle	Clearance angle
55°	0.2 mm	0°	7°

to its hardness is only second to diamond, the cubic boron nitride tools (CBN), polycrystalline diamond tools (PCD), and polycrystalline diamond compact tools (PDC) are typically high-hardness tool materials and are selected as investigated subjects. The geometric parameters of the turning tool are shown in Table 2, and the thickness of the cutting edge is 0.8 mm.

2.2 Experimental design and measurement

The turning experiments were conducted on a CY-K410n CNC lathe, where the auxiliary clamping tooling and the force measuring auxiliary tooling, experimental setup as

Fig. 2 Experimental setup

(a) Auxiliary tooling

(b) Processing lathe
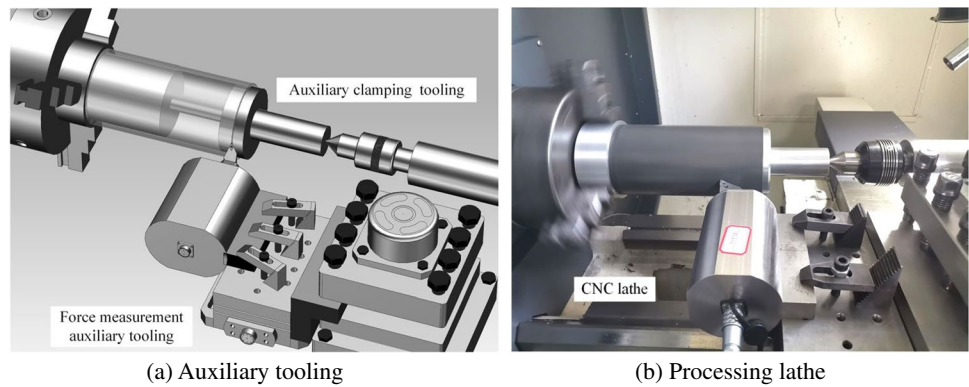
Table 3 Turning parameters for the analysis of cutting performance

No	Cutting speed v (m/min)	Feed rate F (mm/rev)	Depth of cut a_p (mm)	Frequency f (kHz)	Amplitude A (μm)	Tool
#1	60	0.03	0.10	20	3	PDC/CBN/PCD
#2	30	0.05	0.05	30	3	

Table 4 Test parameters for the effect of ultrasonic amplitude on tool wear

No	Cutting speed v (m/min)	Feed rate F (mm/rev)	Depth of cut a_p (mm)	Frequency f (kHz)	Amplitude A (μm)
#3	30	0.03	0.10	20	1/3/5/7
#4	15	0.05	0.05	20	

seen in Fig. 2. Before turning tests, the ultrasonic amplitude was measured and calibrated with the LK-H020 vibrometer to ensure that the amplitude was the same and constant during machining. The cutting force was measured and collected by Kistler 9257B multicomponent dynamometer. In this study, the natural frequency of the dynamometer was 2 kHz, which was smaller than the ultrasonic vibration frequency applied for turning experiments. As noted by other researchers [33, 34], there were no reported investigations using a dynamometer of the same frequency as the ultrasonic vibration. After that, the average cutting force measured by the Kistler dynamometer was used for analysis [35].

As presented in Table 3, turning experiments were performed on SiC_f/SiC ceramic matrix composites using PDC, CBN, and PCD tools to investigate the tool performance in different conditions: conventional turning (CT), ultrasonic vibration-assisted turning (UVAT), and ultrasonic vibration-assisted turning with water cooling (W-UVAT). No coolants were used in CT and UVAT. Based on the preferred tool, to analyze the effect of ultrasonic amplitude on tool wear, the single-factor experiments shown in Table 4 are designed. And the parameters of Table 5 are used to investigate the effect of material removal volume on tool wear, whose purpose was to analyze the mechanism of tool wear further. It should be noted that the removed material volume for test #1 and test #3 was about 250 mm^3, while the volume for test #2 and test #4 was about 125 mm^3.

After turning tests, the 2D surface roughness R_a, the 3D roughness S_a, and the tool wear were scanned and measured with an Alicona Infinite Focus G4 optical 3D scanner. The surface morphology of tool wear was measured by a TESCAN MIRA3 scanning electron microscope. Basically, it was worth noting that the measurement of S_a in the existing literature was on a single yarn, which could only take into account the topography of the fibers and did not consider the complex profile information of the entire machined surface. Therefore, in this work, the measurement of S_a was on a relatively large area.

Table 5 Test parameters for the effect of material removal volume on tool wear

No	Cutting speed v (m/min)	Feed rate F (mm/rev)	Depth of cut a_p (mm)	Frequency f (kHz)	Amplitude A (μm)	Material removal volume V (mm^3)
#5	15	0.03	0.06	20	3	50/100/150/200/250/300/350/400/450/500

3 Tool wear volume

The traditional evaluation standard of tool wear is the width of the flank wear area, *VB*, as presented in Fig. 3 [36]. As shown in Fig. 4, on the basis of trial cutting with PDC tools, it is found that the wear is severe. According to the topography of the worn tools, it is greatly concentrated in the nose area and the deputy flank, and the wear surface approximates a plane. At the equal time, the tool also has a certainly worn angle along the rake face direction. Tool wear is manifested as the removal of tool material over a larger volume of space.

For the tools with linear cutting edge, *VB* can represent tool wear volume well. But for the tools with rounded cutting edge, the same *VB* may represent different wear volumes [16]. At the same time, *VB* is also the traditional blunt standard for tool failure. In actual processing, provided that the failure of the tool is caused by the crushing of the cutting edge, *VB* has not yet reached the blunt standard, resulting in misjudgment and economic loss [17]. Tool wear volume is simple, intuitive, and easy to measure and calculate, which can not only make up for the shortcomings of traditional standard of tool wear and failure but also be more appropriate to describe the essence of material migration for tool wear.
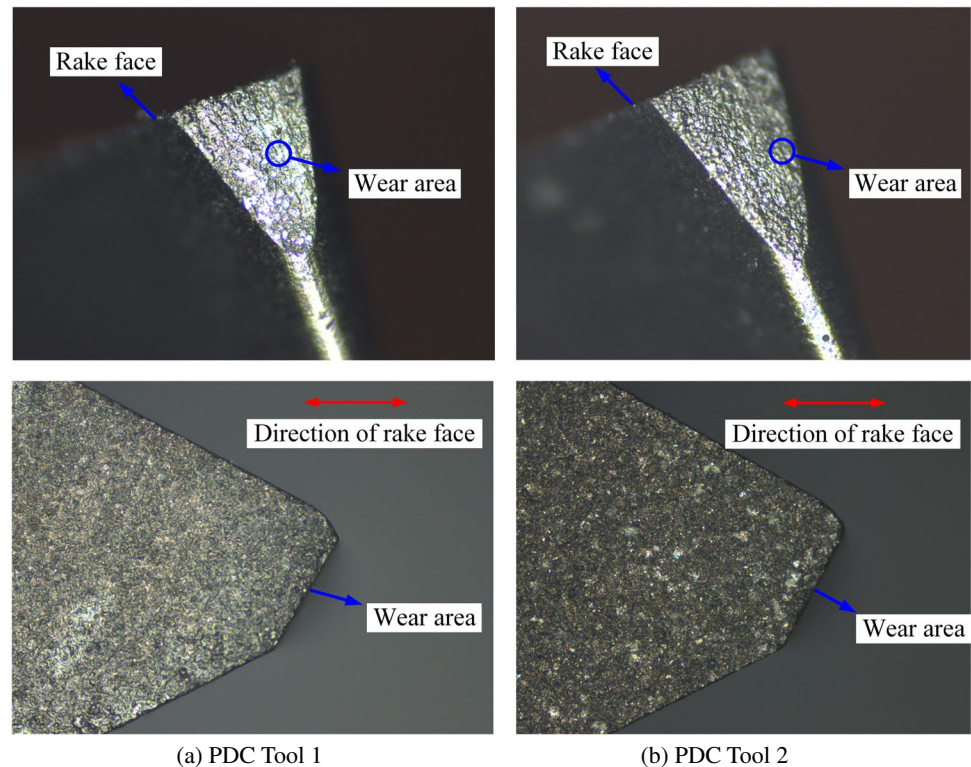
Fig. 3 Flank wear area
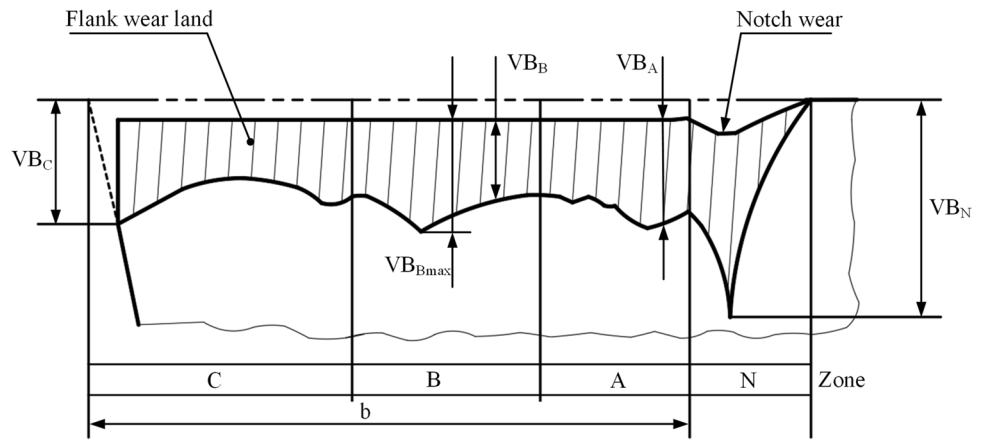
Fig. 4 Topography of the worn tools

(a) PDC Tool 1　　　　　(b) PDC Tool 2

According to the observed features, the area of the tool nose can be simplified into an inverted conical model (Fig. 5). Based on the geometric parameters of the turning tool, the solid model is established in the modeling software. To simplify the model, it merely needs to establish the model that the area with abrasive grains, as shown in the red area of Fig. 5. Thereafter, the VB_{max}, LR_{max}, θ, and L_W parameters are measured by the optical 3D scanner. VB_{max} is the maximum width of the flank wear face (Fig. 6a), and LR_{max} is the maximum distance from the worn edge of the rake face to the tool nose (Fig. 6b). ε_r is the tool nose angle. θ is the angle between the worn edge of the rake face and the long diagonal side of the upper surface of the tool. L_W is the distance from the lowest point of the tool wear surface to the worn edge of the rake face. μ is the angle between the tool wear surface and the rake surface, and its calculation method is shown as Eq. (1):

$$\mu = \arcsin(VB_{max}/L_W) \qquad (1)$$

Figure 7 shows the calculation method of tool wear volume. The datum plane 1 is perpendicular to the rake face and passes through the worn edge. Based on the above measured parameters, the datum plane 1 is established in the modeling software, as shown in Fig. 7a. Taking the worn edge on the rake face (L_{EF}) as the rotation axis and with 90°-μ as the rotation angle, rotate the datum plane 1 to obtain the datum plane 2, as seen in Fig. 7b. Afterward the models are trimmed based on the datum plane 2, which can obtain a model of the worn area. Finally, the tool wear volume is obtained using the function of the volume calculation in the modeling software, which will conveniently, quickly, and accurately get the tool wear volume V_W. In addition, the parameters defined in Section 3 are shown in Table 6.

4 Comparative analysis of tool performance

4.1 Primary analysis of turning tool

Figure 8 presents the turned surface topography obtained by UVAT of SiC$_f$/SiC ceramic matrix composites with the CBN tools, taking the parameters of Table 3. The 3D
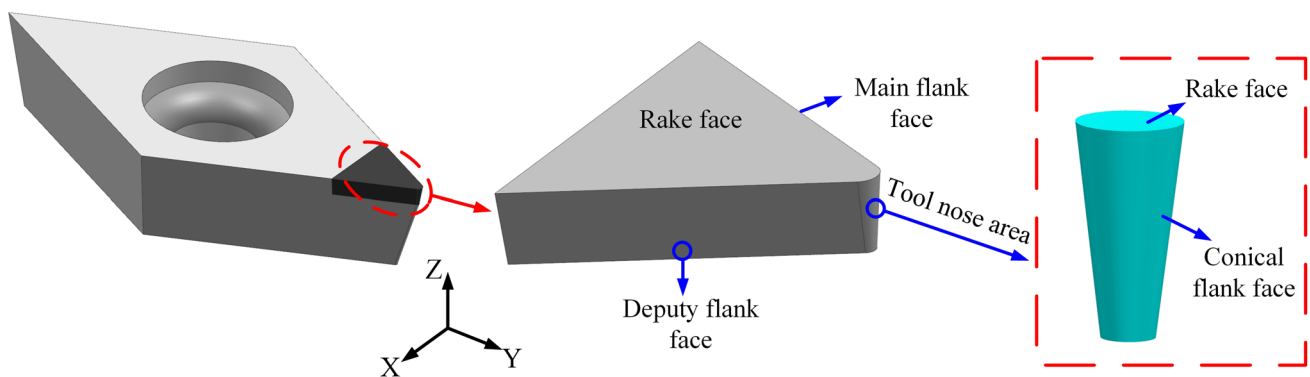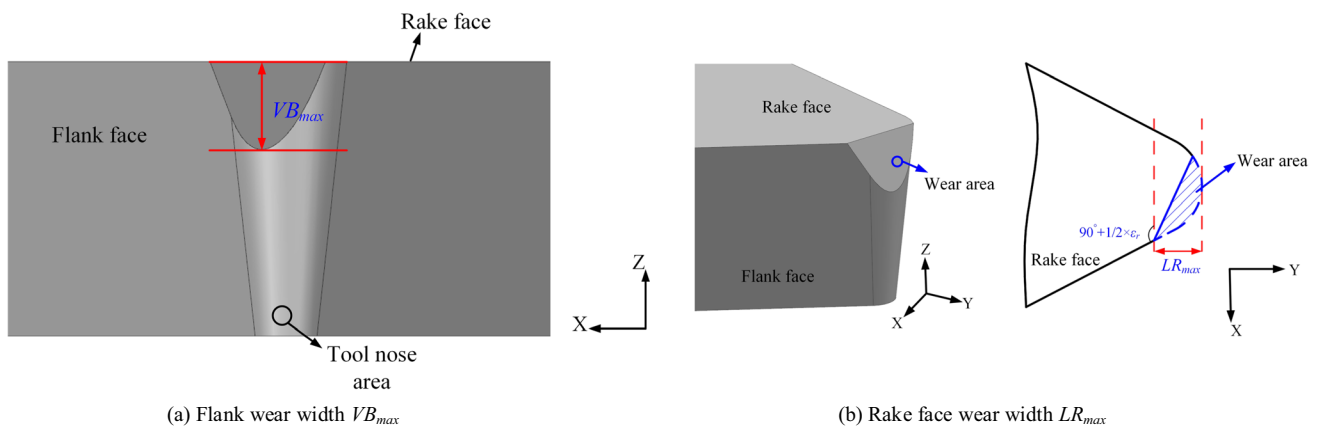

Fig. 5 Conical flank face

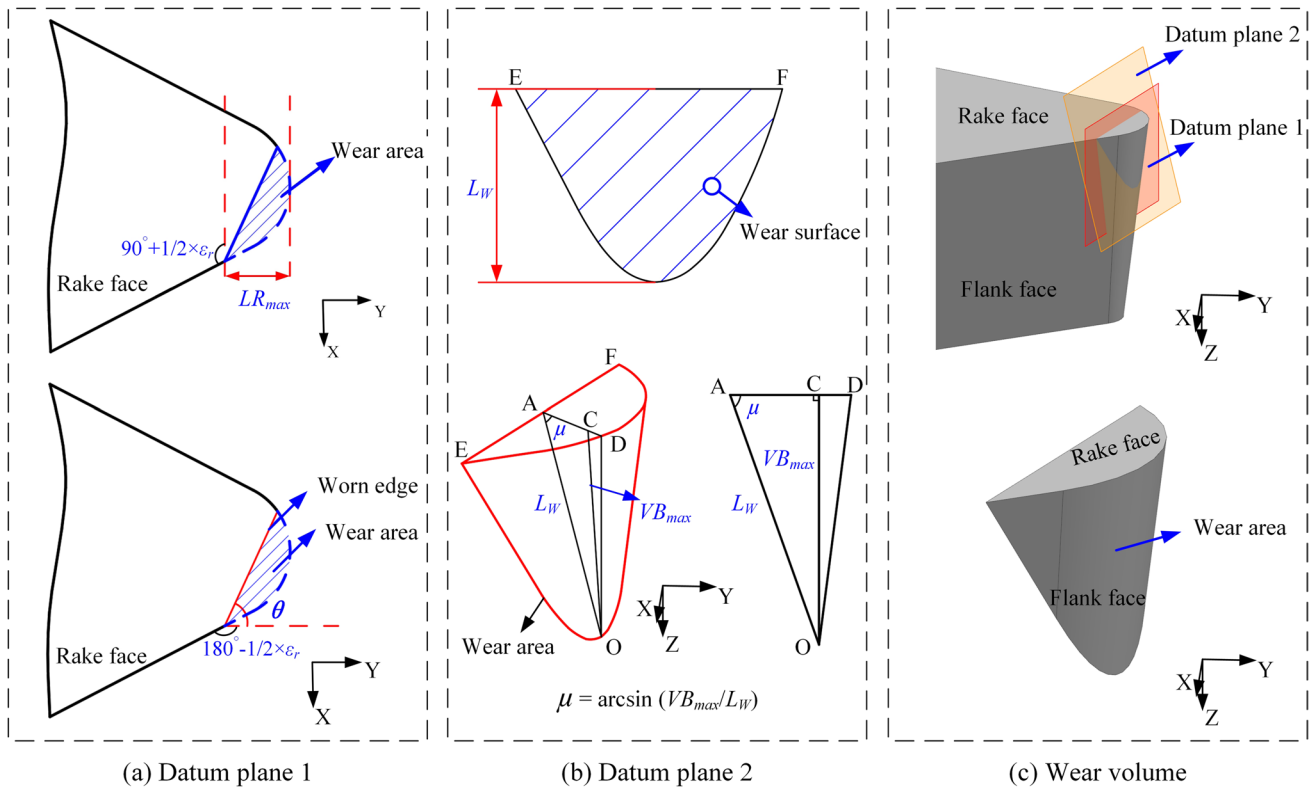(a) Flank wear width VB_{max} (b) Rake face wear width LR_{max}

Fig. 6 Tool wear width

| (a) Datum plane 1 | (b) Datum plane 2 | (c) Wear volume |

Fig. 7 Calculation method of the tool wear volume

Table 6 Defined parameters in Section 3

Parameter	Definition
VB	The width of flank wear area (mm)
VB_{max}	The maximum width of flank wear area (mm)
LR_{max}	The maximum distance from the worn edge of the rake face to the tool nose (mm)
ε_r	Tool nose angle (°)
θ	The angle between the worn edge of the rake face and the long diagonal side of the upper surface of the tool (°)
L_W	The distance from the lowest point of the tool wear surface to the worn edge of the rake face (mm)
μ	The angle between the tool wear surface and the rake surface (°)
V_W	Tool wear volume (mm³)

topography can display the variation of the contour height of the machined surface according to different colors. As can be clearly seen in Fig. 8, the colors of the lower and upper regions of the turned surface topography are fairly different, mainly due to the cylindrical shape of the turning workpiece, leading to the scanned surface being a curved surface with a certain radian. Along the feed direction (axial direction), the turned surface of test #1 has a slight difference of the color. It reveals a certain cutter back-off in the turning process with CBN tools. Figure 9 is the topography of the worn CBN tools. It can be seen from Fig. 9a that although the CBN tool did not chip directly, there is considerable wear in the tool flank area. In addition, a slight edge chipping was resulted along the worn edge of the rake face.

The CBN tool has created a severe edge chipping at the beginning of processing, which has resulted in almost no change in the profile height of the turned surface along the feed direction, as shown in Figs. 8b and 9b. The test was repeated for two times, and the CBN tool all generated serious edge chipping. Figure 10 shows the variation of cutting force signal during this process, and it indicates that the tool is in contact with the workpiece for an exceedingly short time before severe edge chipping. After severe edge

(a) Test #1 (b) Test #2
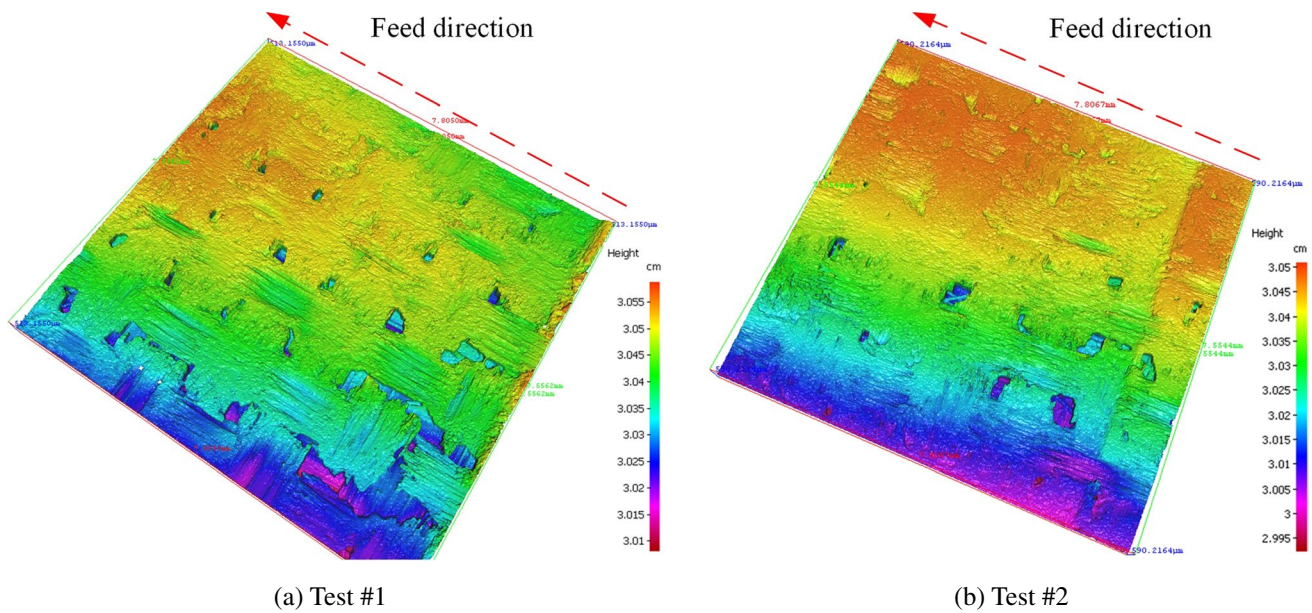
Fig. 8 Surface topography of turning with CBN tools

Fig. 9 Topography of the worn CBN tools


(a) Test #1 (b) Test #2
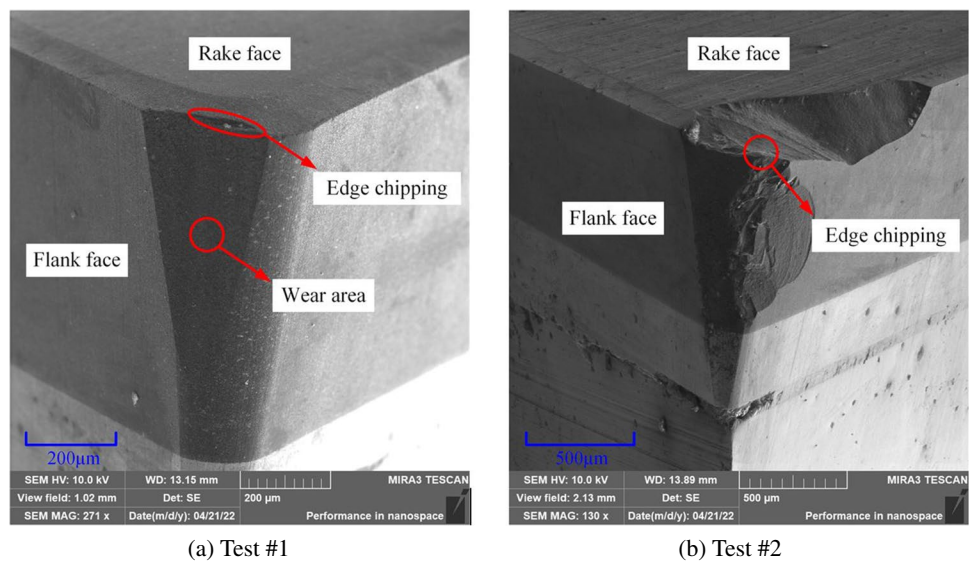
chipping, it is in a state of incomplete contact with the workpiece, and the force value at this stage is close to 0. The cutting force in the X direction is smaller than that in the Y and Z directions, leading to the force signal in the X direction being covered during acquisition (Fig. 10a). As seen in Fig. 10b, the X direction has the signal of the cutting force, but it is very small.

From the analysis of the cutting force signal, it can be seen that the contact time is less than 1/5 of the processing time, which means that the CBN tool is not one-time edge chipping. However, the process of slight edge chipping to severe edge chipping results in rarely slight

contact between the tool and the workpiece on the stage of incomplete contact. Additionally, it can be found that great instantaneous cutting force is generated when the tool cut into the workpiece, and the moment from no-load to heavy load may be the main factor for the edge chipping. The initial edge chipping leads to multiple cracks on the cutting edge of the CBN tool. With the action of cutting force in machining, the cracks extend and expand, resulting in more severe edge chipping. On the contrary, no serious edge chipping occurred when the parameters of test #1 were used for machining, and just slight edge breakage was produced on the worn edge of the rake face. It is mainly

Fig. 10 Cutting force signal of turning with the CBN tool
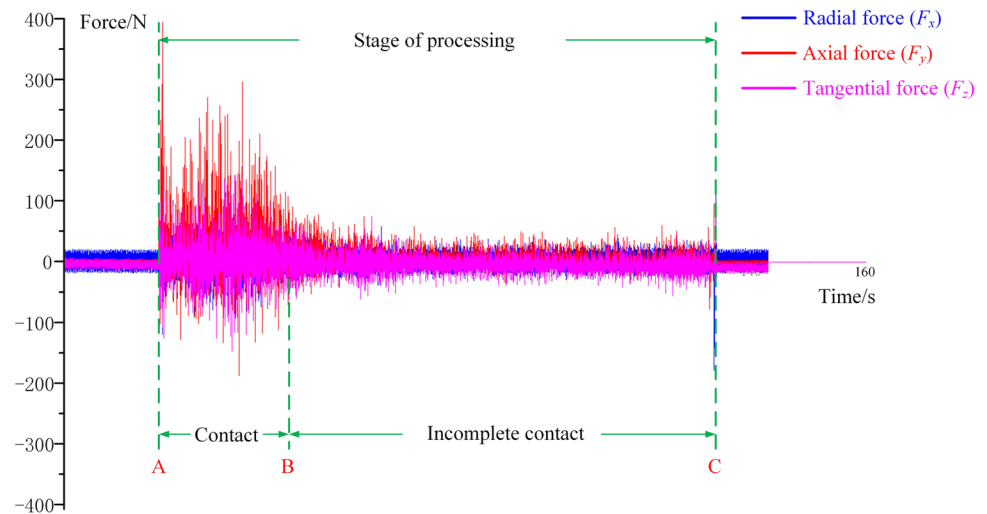

(a) Turning force signal
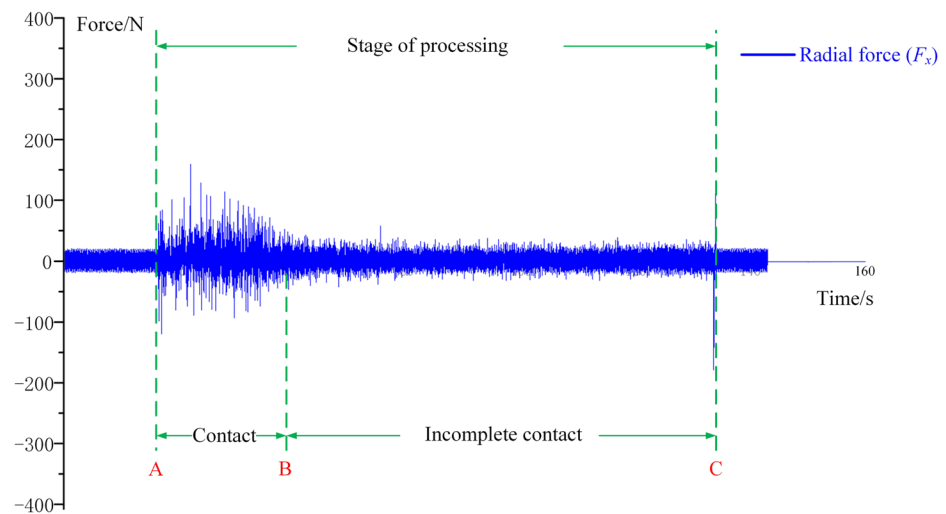
(b) Radial force signal

because the instantaneous cutting force when the tool cut into the workpiece in test #1 is relatively small, which does not reach the limited stress of microcracks or edge chipping. In addition, as the tool wears gradually, the contact mode with the workpiece is changed from point contact to surface contact. The acting area is larger, and the effect of the force on the unit area is reduced. Therefore, it is more difficult to produce the phenomenon of edge chipping.

Many studies have shown that the application of ultrasonic vibration in conventional turning is beneficial to reduce tool wear and improve surface quality [37]. CBN tools would experience more severe wear and poorer surface quality under CT, which may own to the relatively lower hardness of the CBN coating. In this section, the cutting performance of PDC, PCD, and CBN tools in machining SiC$_f$/SiC ceramic matrix composites is analyzed under UVAT. And the results of test #1 were studied because of the serious edge chipping of the CBN tool under test #2.

Figure 11 shows the comparison results of cutting force, tool wear, and surface roughness when turning the workpiece with different tools. As seen in Fig. 11a, the cutting force generated by the PDC tool in the machining process is relatively smaller, while the force caused by PCD and CBN tools is similar. However, the tool wear of the PCD tool is lower than that of the CBN tool. It is mainly attributed to the stronger bonding strength between PCD abrasive grains and higher hardness. In addition, the PDC tool caused relatively minimal tool wear due to the higher wear resistance and bonding strength (Fig. 11b). As shown in Fig. 11c, PDC and PCD tools show similar cutting effects in turning, while the CBN tool has relatively higher surface roughness and poorer cutting performance. This is mainly due to the maximum wear of the CBN tool in turning of SiC$_f$/SiC ceramic matrix composites, which increases the contact length and friction effect between the tool and the workpiece. It causes the fibers to be removed in the form of

Fig. 11 Comparison of tool wear, cutting force, and surface roughness

(a) Cutting force

(b) Tool wear

(c) Surface roughness
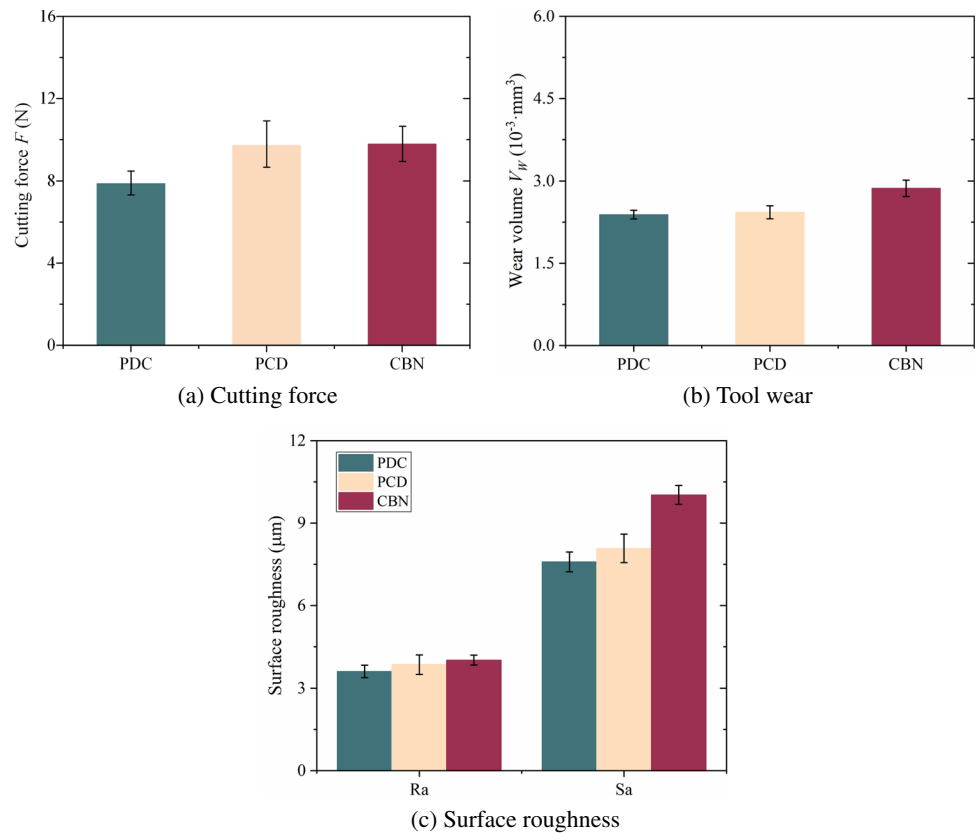
tensile breakage, resulting in relatively more surface defects and poorer surface quality. In conclusion, the CBN tool showed the worst cutting results, and the cutting performance of PDC and PCD tools will be further discussed and analyzed in Section 4.2.

4.2 Tool wear analysis

Experiments of cutting performance are carried out with PCD and PDC tools under divergent machining conditions: CT, UVAT, and W-UVAT. The compared results of the tool wear volume V_W are shown in Fig. 12a. The CT experiments are carried out, and basically, the tool wear caused by the PDC tool is lower than that of the PCD tool. However, in UVAT, the V_W caused by the PCD tool is not much different from that created by the PCD tool. During W-UVAT, PDC tools all showed relatively small tool wear. The essence of the PDC and PCD tool is obtained by pressing polycrystalline diamond powder under ultra-high pressure and ultra-high temperature conditions. However, the difference in the bonding strength of grains and the manufacturing process of tool leads to obvious differences in turning performance, whose external forms are diverse tool wear.

Cutting force is the most important factor in the analysis of tool wear. Figure 12b shows the compared results

of cutting forces when turning SiC$_f$/SiC ceramic matrix composites with PDC and PCD tools under CT, UVAT, and W-UVAT conditions. Among them, the cutting force is the resultant of the average cutting forces in the X, Y, and Z directions. Basically, it can be clearly seen that the PDC tool generates relatively low cutting forces in turning. However, in UVAT, the cutting force generated by the parameters of test #2 is slightly larger than that of the PCD tool. SiC$_f$/SiC ceramic matrix composites are typical anisotropic and heterogeneous materials, and fibers and matrix are not entirely distributed on the workpiece surface. In the meantime, the matrix material and the reinforcing fibers have different hardness, which shows differently removed difficulties during turning SiC$_f$/SiC ceramic matrix composites. Therefore, the difference in the machining position will have a certain influence on the cutting force. The change and magnitude of cutting force during turning have a profound impact on tool wear. It can be seen from Fig. 12b that the cutting force caused by the PDC tool is smaller than that of the PCD tool. Therefore, the PDC tool obtained a relatively lower cutting force when turning SiC$_f$/SiC ceramic matrix composites, resulting in a smaller tool wear. Overall, from the perspective of tool wear, the PDC tool causes the relatively smallest V_W, showing relatively better cutting performance in turning of SiC$_f$/SiC ceramic matrix composites.

Fig. 12 Tool wear and cutting force in CT, UVAT, and W-UVAT

(a) Tool wear (b) Cutting force
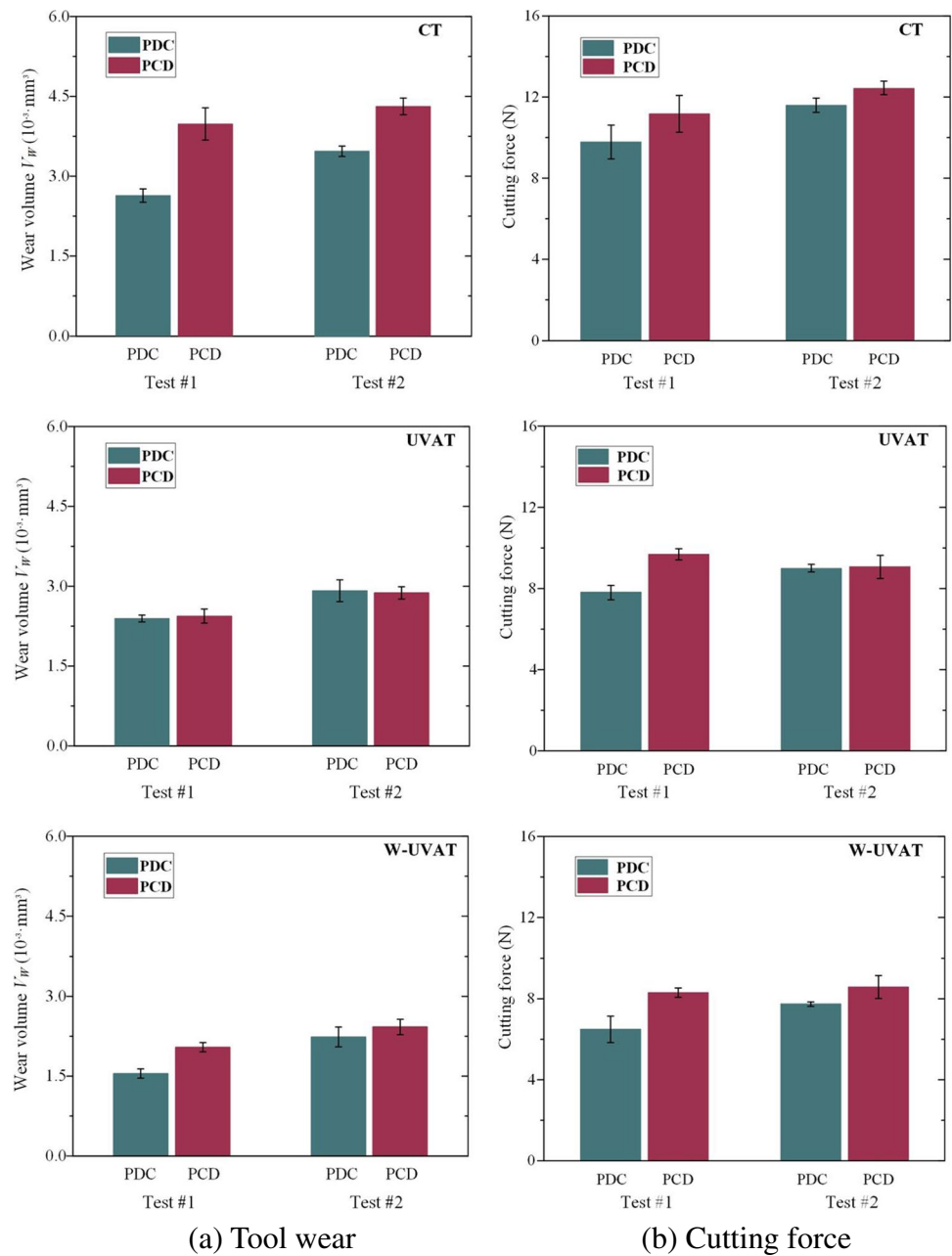
4.3 Machined surface roughness

Using the parameters of Table 3, experiments of turning SiC$_f$/SiC ceramic matrix composites are carried out under three processing conditions: CT, UVAT, and W-UVAT. Figures 13, 14, and 15 show the compared results of the turning surface roughness of diverse tools under different conditions. It can be clearly seen that the 3D surface roughness S_a is higher than the 2D surface roughness R_a, which can be due to S_a being the result of extending a 2D curve to a 3D surface. In the course of the measurement of S_a, the complex profile information of the turned surface, including fiber breakage, matrix pits, hole defects, etc., are comprehensively considered. The SiC$_f$/SiC ceramic matrix composite used in this paper has many prepared hole defects, and the S_a measurement area is relatively large, resulting in the S_a value being greater.

In test #1 of CT, the R_a of the turned surface with the PDC tool is slightly larger than that of the PCD tool, while the S_a is smaller. It may be due to the fact that R_a is measured along a certain direction, resulting in the measurement result being easily affected by the measured position. In test #2 of CT, the R_a and S_a of the turned surface of the PDC tool are all slightly smaller than those of the PCD tool. Basically, in UVAT and W-UVAT, relatively better machining results are obtained by turning SiC$_f$/SiC ceramic matrix composites

Fig. 13 Surface roughness of CT

(a) Test #1 (b) Test #2
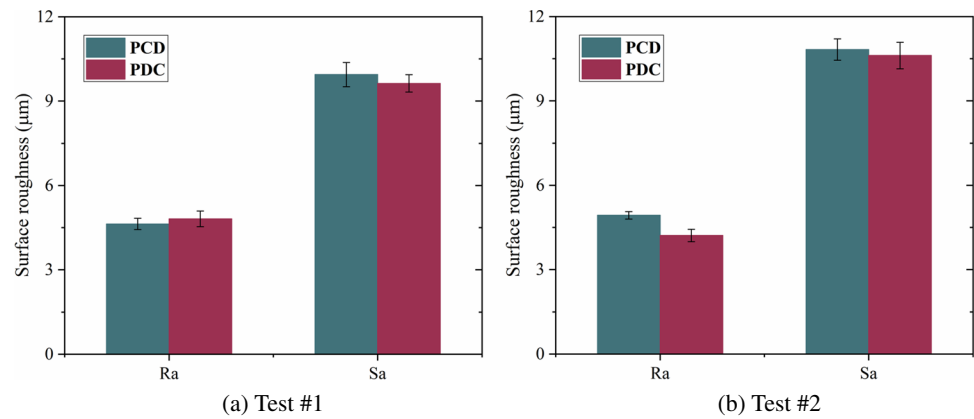
Fig. 14 Surface roughness of UVAT

(a) Test #1 (b) Test #2
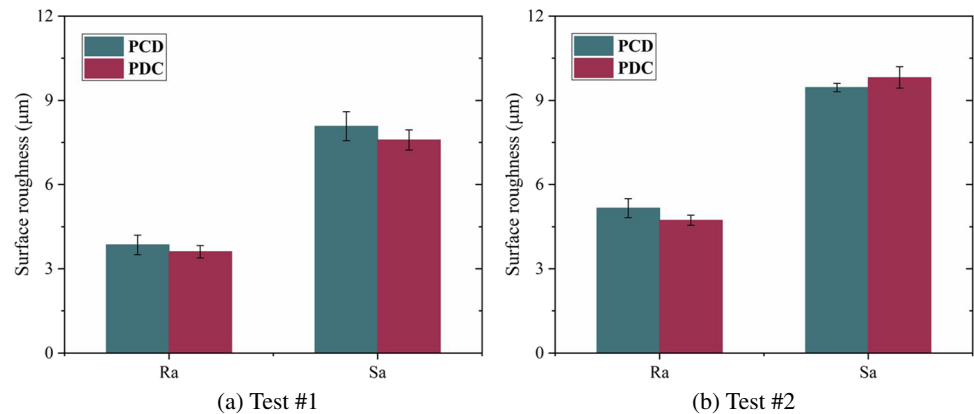
Fig. 15 Surface roughness of W-UVAT

(a) Test #1 (b) Test #2
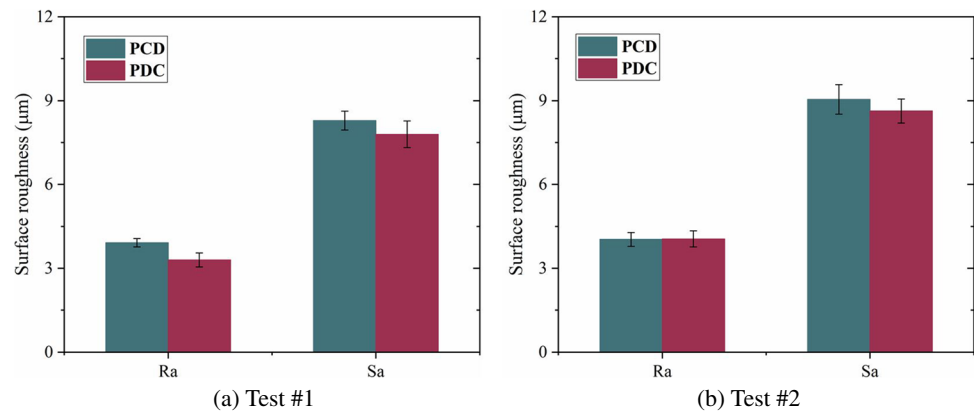
with PCD tools. Nevertheless, in test #2 of UVAT, the S_a of the turned surface obtained by the PDC tool is slightly larger. The immature process of the material preparation can easily lead to more hole defects, or the structural quality is not completely consistent, resulting in the measurement of S_a being affected by the measurement location. In addition, a general belief in many articles is on the detrimental effect of tool wear on surface roughness. Basically, the PDC tool gets relatively low tool wear, which would also be beneficial to obtain relatively better surface roughness, as obtained in Section 4.2. On the whole, under CT, UVAT, and W-UVAT

processing conditions, relatively good R_a and S_a can be obtained using PDC tools.

In the meantime, it can be clearly seen from the above research that the application of ultrasonic vibration and cooling in CT is beneficial to the machining quality, tool wear, and cutting force, which is basically consistent with the conclusions reached by other researchers [38, 39]. Therefore, follow-up studies are carried out under W-UVAT conditions. PDC tool has achieved relatively better turning characteristics, but the tool wear is still serious. Then, PDC tools with the same specification and the cutting edge thickness of 1.6

mm are used for the following research, which can prevent the workpiece from rubbing against the tool matrix when the wear is severe.

5 Tool wear mechanism

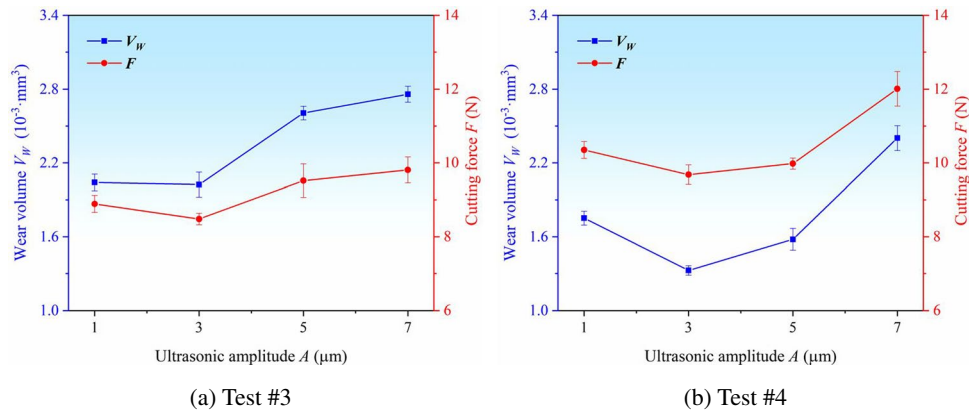## 5.1 Effect of ultrasonic amplitude on tool wear

Figure 16 represents the effect of ultrasonic amplitude on PDC tool wear and cutting force, where the cutting force is the resultant cutting force in the directions of X, Y, and Z. Within the parameters of Table 4, the ultrasonic amplitudes are 1 μm, 3 μm, 5 μm, and 7 μm. In tests #3 and #4, the tool wear volume V_W decreases first and then increases as the increased ultrasonic amplitude, reaching the minimum value when the ultrasonic amplitude $A = 3$ μm. In the meantime, it is obvious that the cutting force has the same tendency, reaching the smallest in $A = 3$ μm.

The cutting force and tool wear are linked to each other. It can be seen from Fig. 17 that ultrasonic amplitude will significantly affect the actual depth of cut in the turning process. When applying the ultrasonic amplitude, the depth

of cut changes dynamically, whose real value varies within $a_p \pm A$ mm, where a_p is the depth of cut, and A is the ultrasonic amplitude. The effect of ultrasonic amplitude on the actual depth of cut will be further analyzed and discussed in Section 5.2. Since the tool movement is a sinusoidal path, the bumpy surfaces would be generated of the same size on the turned surface of the workpiece. Theoretically, on the basis of the same a_p and the cutting width L, the removed material volume by the turning tool is the same when machining with different ultrasonic amplitudes. However, ultrasonic amplitudes would have different effects on the actual depth of cut. The larger the ultrasonic amplitude, the larger the actual maximum depth of the cut, resulting in the instantaneous cutting force may be greater. It may further lead to an increase in the average cutting force.

The ultrasonic impact effect would increase with increasing amplitude, and then the increasing amplitude within a specific range makes the tool-workpiece separation effect more conspicuous, reducing the cutting force. However, with increasing amplitude, the increasing impact effect would increase tool wear due to the high and similar hardness and brittleness of both the tool and workpiece. In addition, the increasing amplitude would influence the stability of the

Fig. 16 The effect of ultrasonic amplitude on the PDC tool wear and cutting force

(a) Test #3 (b) Test #4

Fig. 17 The effect of ultrasonic amplitude on the actual depth of cut
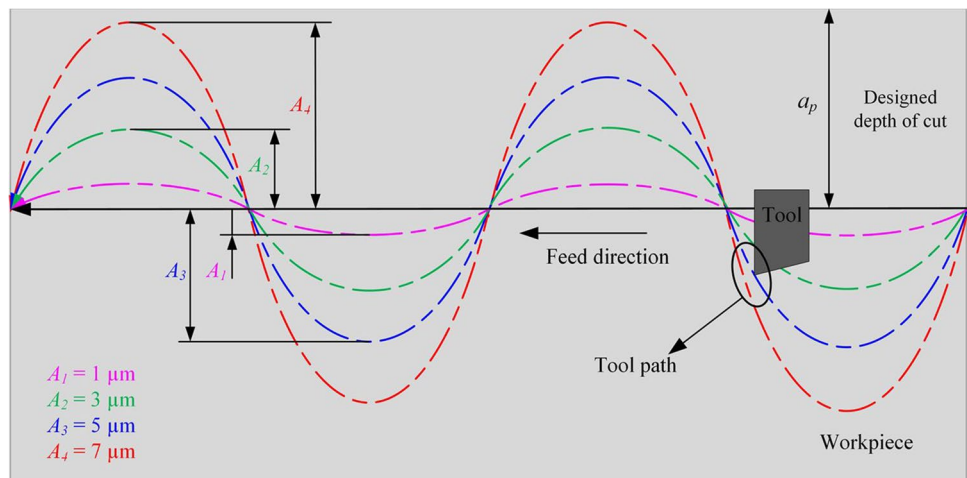
cutting system and machining process resulting in increasing cutting force [40]. It can be seen from Fig. 16 that the cutting force continues to increase as the ultrasonic amplitude increases from 3 to 7 µm. However, the cutting force of $A = 1$ µm is larger than $A = 3$ µm, which can be own to the vibration being extremely small at $A = 1$ µm. The effect of ultrasonic vibration cannot be well reflected, resulting in machining results close to CT. As a result, the cutting force and tool wear volume are all relatively large at $A = 1$ µm.

Basically, the cutting force is positively correlated with tool wear. In a certain range, the cutting force may be increased with the strengthening of the scratching effect between the tool and the workpiece, which further accelerates the spalling of PDC abrasive grains, and the wear becomes larger. On the contrary, the contact area between the tool and the workpiece may increase with the increased wear, causing greater friction, which will significantly increase the cutting force. As seen in Fig. 16, the cutting force and tool wear have the similar trend, and the tool wear and cutting force of the PDC tool are all minima as the amplitude reaches 3 µm.

As shown in Fig. 18, with the increase of ultrasonic amplitude, the turning surface roughness R_a and S_a of the two groups of turning tests first decreases and then increases. The surface roughness is the smallest when the amplitude is 3 µm. Further analysis of Fig. 17 shows that the ultrasonic amplitude will affect the flatness of the workpiece surface while changing the actual cutting depth. The larger the ultrasonic amplitude, the larger the theoretical profile fluctuation of the workpiece surface, which affects the roughness level. The ultrasonic vibration-assisting effect can reduce surface damage and decrease surface roughness to a certain extent. Properly increasing the ultrasonic amplitude is beneficial to improve the inhibition effect of ultrasonic vibration on surface damage. However, excessive ultrasonic vibration will destroy the stability of the machining system and will increase the surface roughness of the workpiece [32]. Large tool wear in machining SiC$_f$/SiC ceramic matrix composites

will also make it difficult to obtain better machined surface roughness. From the previous analysis, it can be seen that the tool wear reaches the minimum when $A = 3$ µm. These indicate that in W-UVAT, choosing the appropriate ultrasonic amplitude is beneficial to reduce the surface damage and improve the machining effect.

5.2 Tool wear mechanism analysis

The tool cutting edge angle K_r is the angle between the projection of the main cutting edge on the base plane and the direction of the feed rate. The tool minor cutting edge angle K_r' is the angle between the projection of the deputy cutting edge on the base plane and the opposite direction of the feed rate. Figure 19 is a schematic diagram of cutting a workpiece with different K_r and K_r' by a tool with the identical specification. The different K_r and K_r' affect the contact position between the tool and the workpiece when the tool cuts into the workpiece, resulting in a change in the position of tool wear. As presented on the right side of Fig. 19, this paper uses a tool with the nose angle $\varepsilon_r = 55°$ and the tool cutting edge angle $K_r = 90°$. The contact position of the tool and the workpiece concentrates on the nose area and the deputy flank. In the meantime, the main cutting edge also has contact with the transitional surface of the workpiece.

However, the hardness of SiC$_f$/SiC ceramic matrix composites is extremely high. To prevent the tool from wearing too fast, the depth of cut selected in the research is smaller than the nose radius of the tool. In the meantime, the main flank of the tool does not coincide with the cutting plane. On the contrary, it contains a certain negative angle β between the cutting plane and the main flank in turning, as shown in Fig. 20. The contact area between the main flank and the transition surface of the workpiece is small, which is own to the design of tool structure, and it reduces the friction between tool and workpiece. In fact, when $K_r = 90°$ and the depth of cut is small, there is almost no contact friction between the main cutting edge and the workpiece. Basically, these result in no

Fig. 18 The effect of ultrasonic amplitude on surface roughness
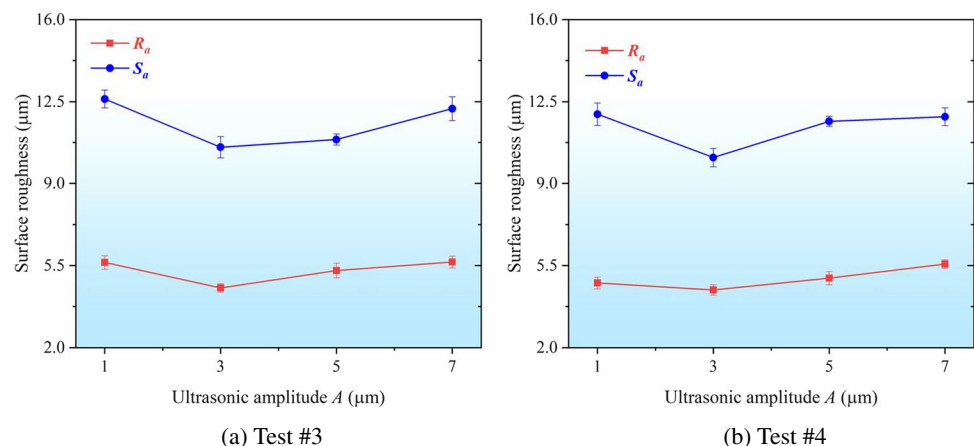

(a) Test #3

(b) Test #4

Fig. 19 Cutting edge angle

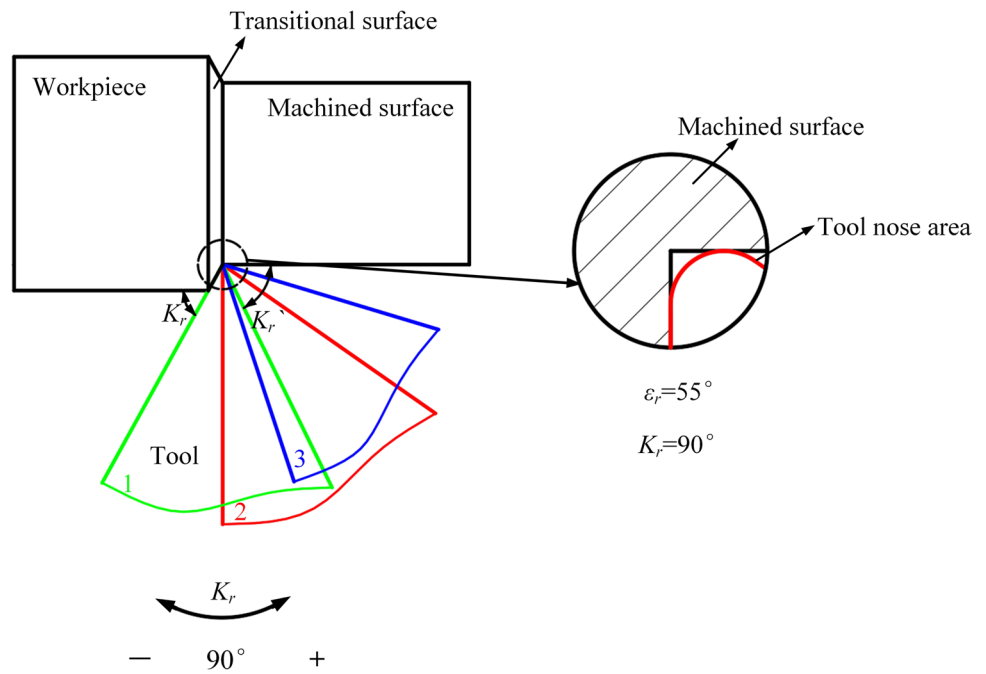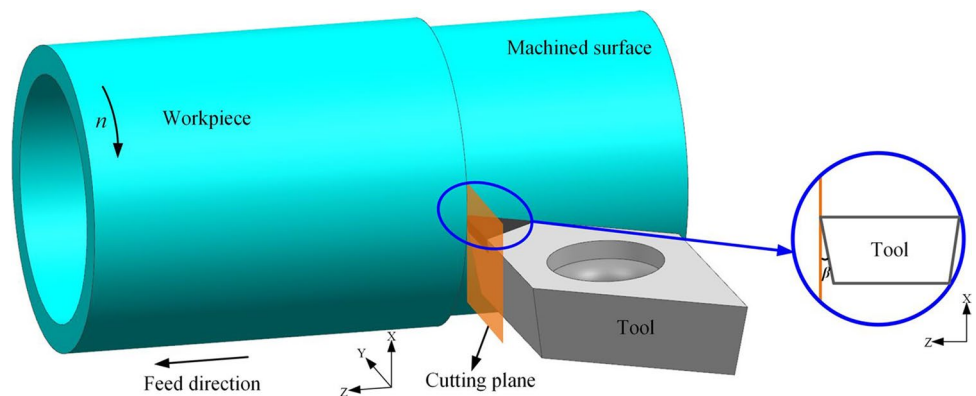**Fig. 20** Angle β between the cutting plane and the main flank

wear on the main cutting edge except for its own manufacturing defects. Figure 21 clearly shows the conditions of tool wear when the ultrasonic amplitude is 3 μm, and the wear is concentrated in the area of the tool nose and the deputy flank.

As shown in Fig. 22, a Cartesian coordinate system was established to describe the spatial position and cutting direction, which was consistent with the coordinate movement of the CNC lathe. The X, Y, and Z directions of the coordinate axis were the cutting depth direction, cutting direction, and feeding direction.

To expound the kinematics for processing, a point P on the tool tip was used to describe the kinematic equation, and a polar coordinate system (R-θ-Z in Fig. 22) was established on the workpiece. The cutting radius R_c in CT is a fixed value, which can be expressed as:

$$R_c = r_m - a_p \tag{2}$$

where r_m is the radius of the machined surface in the last cutting stage and a_p is the depth of cut. Consequently, the instantaneous location equation of this point in CT is

$$\begin{cases} R = r_m - a_p \\ \theta = \omega_n \bullet t = \dfrac{n\pi t}{30} \\ Z = f_z \bullet t \end{cases} \tag{3}$$

where n is the spindle speed, ω_n is the spindle angular velocity, f_z is the feed speed, and t is the cutting time.

The radial UVAT is the application of radial ultrasonic vibration in CT. Therefore, the instantaneous location equation of the P point can be expressed as:

Fig. 21 Worn PDC tools when $A = 3$ μm
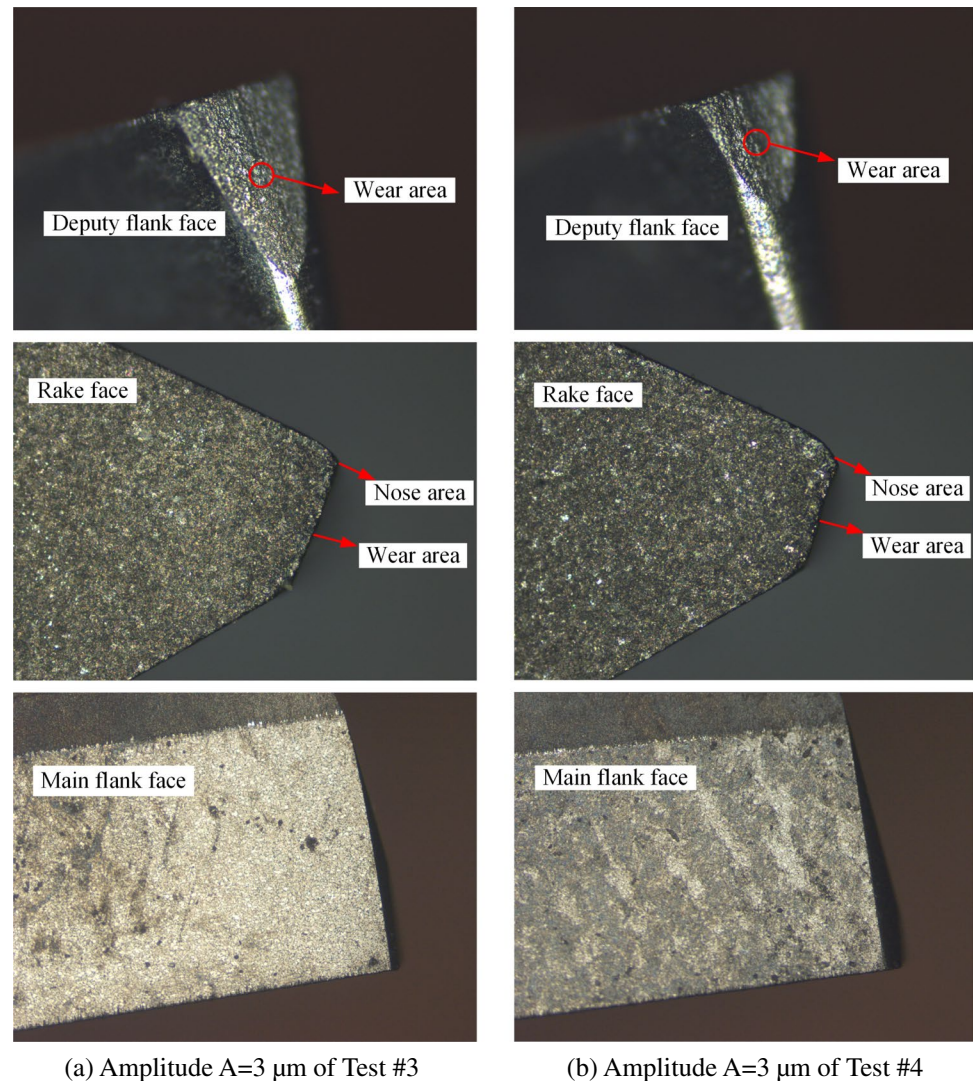
(a) Amplitude A=3 μm of Test #3   (b) Amplitude A=3 μm of Test #4

$$\begin{cases} R = r_m - a_p + A\sin(2\pi f t) \\ \theta = \omega_n \bullet t = \frac{n\pi t}{30} \\ Z = f_z \bullet t \end{cases} \quad (4)$$

where A is the ultrasonic amplitude and f is the ultrasonic frequency.

The UVAT is different from CT in that the motion of the tool tip P point is a combination of three actions: rotational movement relative to the workpiece, axial feed, and radial ultrasonic vibration (Eqs. (3) and (4)). Figure 23 presents the tool path of CT and UVAT. And Fig. 24 shows the accumulation of cutting workpiece powders on the PDC tools during CT and W-UVAT. Obviously, in CT, the tool is in constant contact with the workpiece, whose depth of cut remains unchanged during machining, resulting in a large number of powders accumulating on the cutting position and the rake face. The high pressure generated in the cutting zone during machining causes part of the powders to remain in the worn area. The cutting workpiece powders contain hard SiC fibers and SiC matrices, possibly even mixed with partially spalled abrasive grains of polycrystalline diamond, which may play a role in grinding during the contact between the workpiece and the tool, aggravating the tool wear.

In radial UVAT, applying ultrasonic vibration brings the tool into intermittent contact with the workpiece, resulting in a high-frequency dynamic change in the depth of cut of radial UVAT (the frequency is equal to the ultrasonic vibration frequency, and the amplitude is equal to the ultrasonic vibration amplitude). Due to the action of ultrasonic vibration, the cutting radius R changes dynamically during machining [38, 39], which can take away part of the cutting workpiece powders and reduce the working load and cutting heat. Based on that, water cooling can help to wash away broken fibers and matrix powders effectively, thereby avoiding the accumulation of powders and workpiece material's remains to the tool's cutting edge. However, the tool is still continuously subjected to dynamic load and mechanical
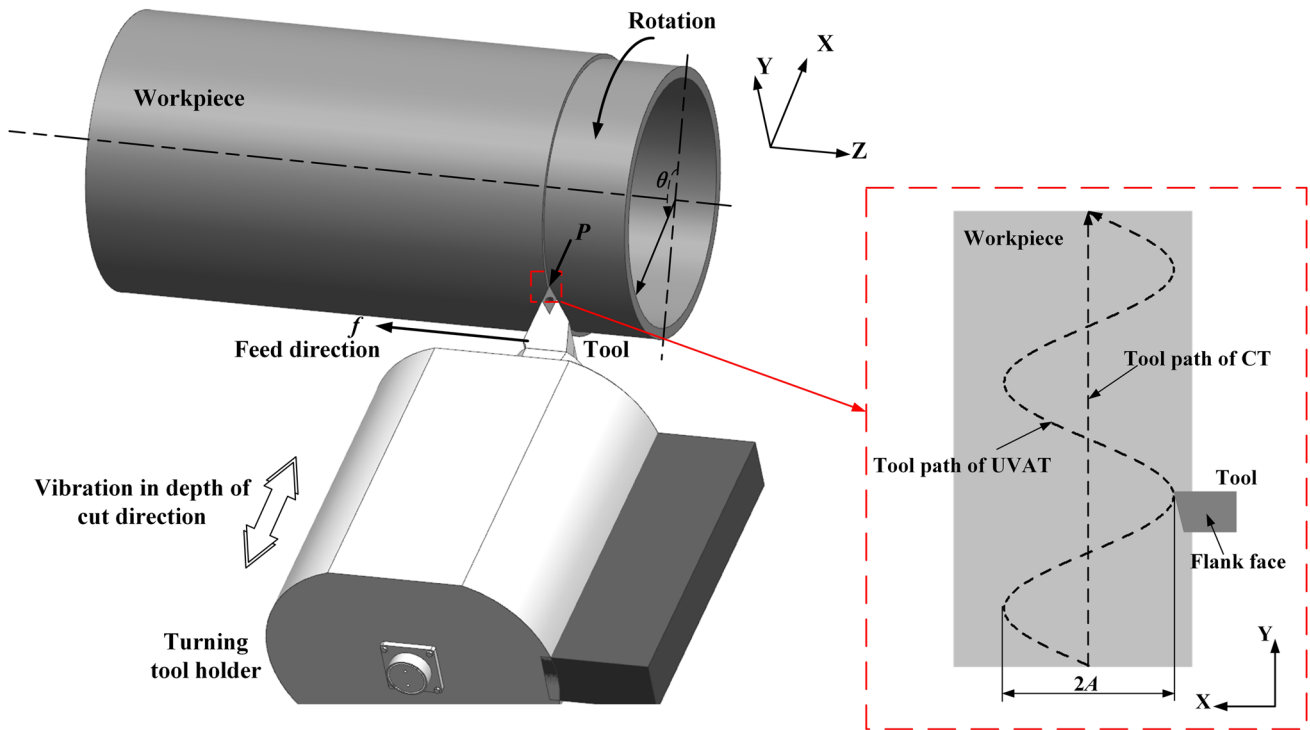
Fig. 22 Schematic of the UVAT method
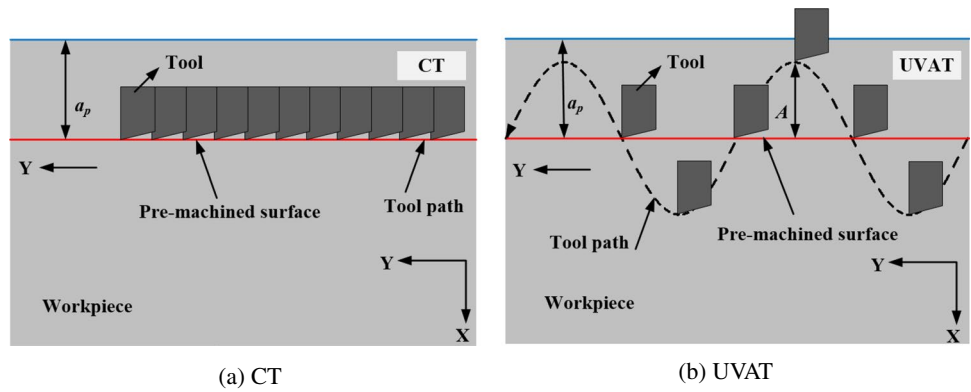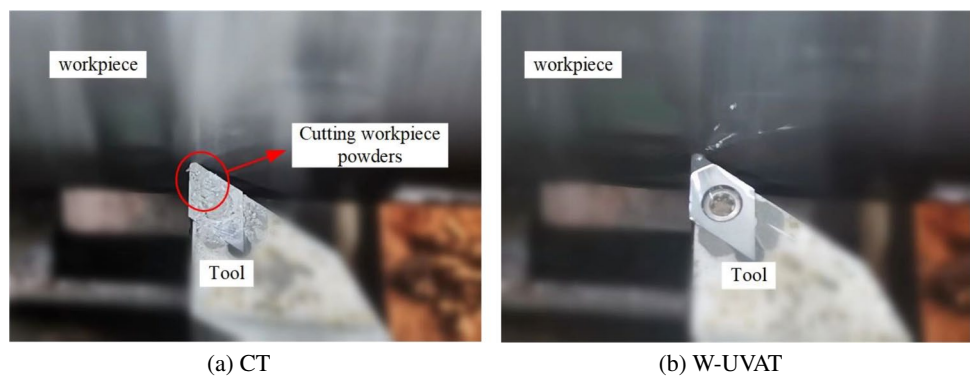

Fig. 23 Tool path of CT and UVAT

(a) CT　　　　　　　　　　　　　　　　(b) UVAT

Fig. 24 Accumulation of cutting workpiece powders

(a) CT　　　　　　　　　　　　　　　　(b) W-UVAT

scratching of fibers during processing, which will cause rapid spalling of the polycrystalline diamond grains. As a result, gradually, the tool will wear out with the increased machining time and material removal volume.

To further investigate the wear behavior of PDC tools in turning, the parameters of Table 5 are used to study the effect of material removal volume on tool wear volume. The results of the PDC tool wear curve are shown in Fig. 25. As the volume of material removed increases, the tool wear volume V_W increases almost linearly. The hardness of SiC$_f$/SiC ceramic matrix composites is second to diamond. When the material removal volume is 50 mm^3, the V_W is 1.325×10^{-3} mm^3, which indicates that the initial wear of the PDC tool during turning is severe. The maximum wear width of the tool specified in the international standard is 0.6 mm. While the material removal volume exceeds 300 mm^3, VB_{max} will exceed 0.6 mm, and V_W will be over 3.060×10^{-3} mm^3. It can be seen that even if PDC tools are used to turn SiC$_f$/SiC ceramic matrix composites, there will still be severe tool wear.

The change in cutting force signal by turning SiC$_f$/SiC ceramic matrix composites during the first 6.4 s (parameters of Table 5) is presented in Fig. 26. The average value of the cutting force in the un-machined stage is close to 0. Meanwhile, due to the cutting force increasing abruptly from the no-load to load stage and the high hardness of the workpiece, significantly initial wear of the PDC tool has been created. In a short time, the larger initial tool wear makes the actual cut depth slightly smaller, resulting in the cutting force being smaller than the suddenly increased value from the no-load to load stage. From the tool wear curve, when the $VB_{max} \leq 0.6$ mm, the maximal material removal volume for the PDC tool is approximately 300 mm^3. Therefore, Fig. 27
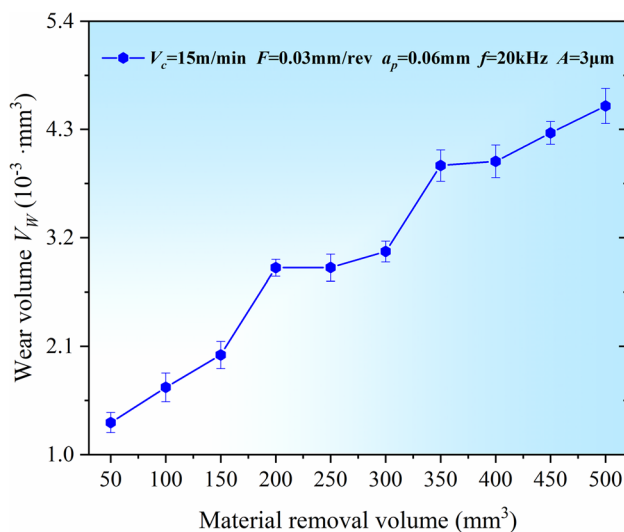

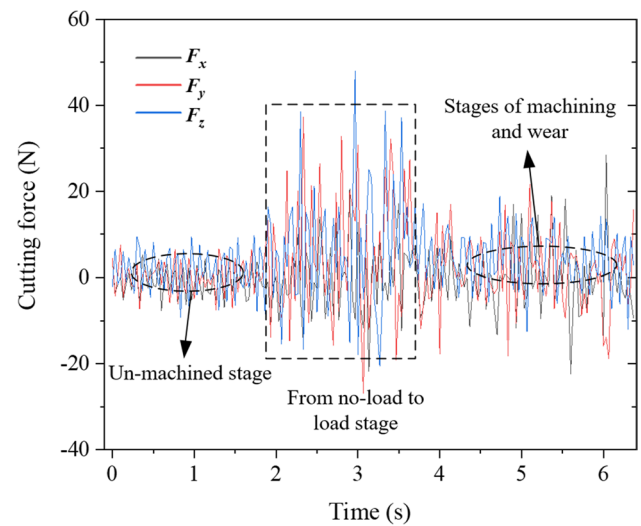**Fig. 26** Analysis of cutting force signal

investigates the variation of radial force (X), axial force (Y), tangential force (Z), and resultant force F as the material removal volume increases from 50 to 300 mm^3. With the increased material removal volume, the cutting force increases gradually. Still, the radial force is relatively slow, which may be for the small depth of cut or the tool wear. The initial contact between the workpiece and the tool is a point contact, which will become a surface contact after wearing. It will increase the contact area and friction between the tool and workpiece, thereby increasing tool wear, as seen in Fig. 28. The cutting force and tool wear will continue to increase over the tool life. As long as the workpiece and tool are not entirely separated, the tool wear will increase with the increased material removal volume even if the cutter is
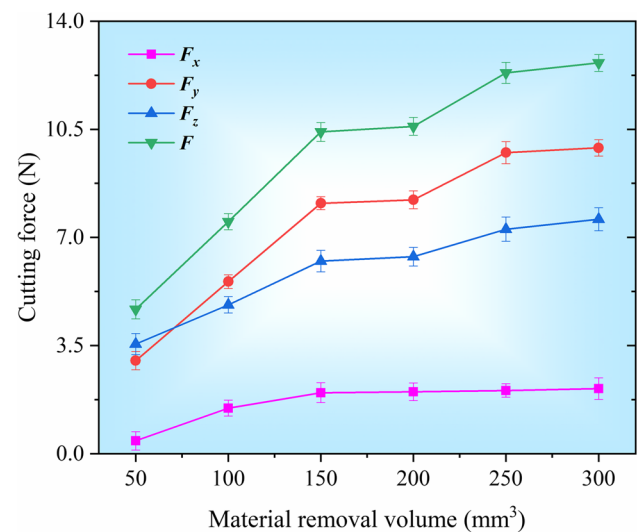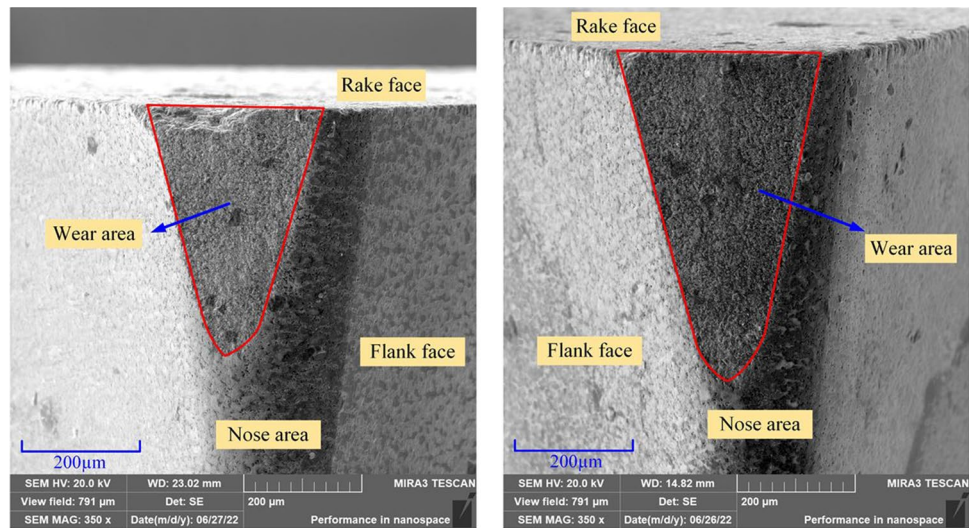

Fig. 25 Tool wear curve

Fig. 27 The effect of tool wear on cutting force

Fig. 28 Worn PDC tools with different material removal volumes

(a) Material removal volume is 100 mm³   (b) Material removal volume is 300 mm³

severely back-off. And beyond tool life, the effect of material removal on tool wear may dominate during the turning of SiC_f/SiC ceramic matrix composites.

In the meantime, Fig. 28 reveals the removal of tool material is a significant change in the volume of space when the tool wears during the turning of SiC_f/SiC ceramic matrix composites. As the volume of material removed increases, it is accompanied by rapid spalling of the abrasive grains, which can be attributed to the high hardness of the SiC_f/SiC ceramic matrix composites and the bonding strength between grains. PDC tool is made by sintering diamond powder and cemented carbide substrate under ultra-high pressure and ultra-high temperature conditions, which has a certain bonding strength between the abrasive grains. Due to the relatively lower bonding strength between grains and the high and similar hardness of material-tool, the grains of the PDC tool are worn gradually in turning of SiC_f/SiC ceramic matrix composites and spalled rapidly with the increased material removal volume. It can be seen that the spalling of the PDC tool (tool wear volume) increases significantly as the removed material volume increases from 100 to 300 mm³, as shown in Fig. 28.

6 Conclusion

In this work, to solve the machining problem of the difficult-to-cut SiC_f/SiC ceramic matrix composites, the ultrasonic vibration-assisted machining technique was used in turning. To conduct a series of research on turning this kind of material, the calculated method of the tool wear volume, the cutting performance, and the wear mechanism should be studied and analyzed first. Based on the results and analysis, the following conclusions can be drawn:

(1) Due to the extremely high hardness of SiC_f/SiC ceramic matrix composites, CBN tools are prone to edge chipping or difficult to obtain satisfactory machining results, while turning with PDC tools in CT, UVAT, and W-UVAT can achieve somewhat lower tool wear and smaller cutting force and get relatively better surface quality. In addition, applying ultrasonic vibration and water cooling in CT with the proper tool is beneficial to improve machining characteristics.

(2) With increasing ultrasonic amplitude A, tool wear volume V_W decreases first and then increases within the experimental parameters. For better-turned surface roughness, lower tool wear, and a smaller cutting force, an ultrasonic amplitude of 3 μm is recommended in turning of SiC_f/SiC ceramic matrix composites with a frequency of 20 kHz.

(3) Due to the high and similar hardness of SiC_f/SiC ceramic matrix composites and cutting tools, the abrasive wear of grains is the main wear mechanism of the PDC tool in turning. And the spalling of polycrystalline diamond abrasive grains is the primary wear form with a relatively lower bonding strength between grains.

At present, the ultrasonic vibration-assisted turning of SiC_f/SiC ceramic matrix composites is still at the stage of fundamental research. Further research is required in terms of optimization of the geometric tool parameters, optimization of the machining parameters, and the material removal mechanism, etc.

Declarations

References

1. Paulmier T, Balat-Pichelin M, Queau DL (2005) Structural modifications of carbon–carbon composites under high temperature and ion irradiation[J]. Appl Surf Sci 243(1–4):376–393
2. Ohnabe H, Masaki S, Onozuka M, Kaoru M, Tadashi S (1999) Potential application of ceramic matrix composites to aero-engine components[J]. Compos A Appl Sci 30(4):489–496
3. Wang PR, Liu FQ, Wang H, Li H, Gou YZ (2019) A review of third generation SiC fibers and SiC$_f$/SiC composites[J]. J Mater Sci Technol 35(12):2743–2750
4. Wu DF, Wang YW, Shang L, Pu Y, Gao ZT (2016) Thermo-mechanical properties of C/SiC composite structure under extremely high temperature environment up to 1500° C[J]. Compos B Eng 90:424–431
5. Kumar J (2013) Ultrasonic machining—a comprehensive review[J]. Mach Sci Technol 17(3):325–379
6. Diaz OG, Luna GG, Liao Z, Axinte D (2019) The new challenges of machining ceramic matrix composites (CMCs): review of surface integrity[J]. Int J Mach Tool Manu 139:24–36
7. Sonia P, Jain JK, Saxena KK (2021) Influence of ultrasonic vibration assistance in manufacturing processes: a review[J]. Mater Manuf Process 36(13):1451–1475
8. An QL, Chen J, Ming WW, Chen M (2021) Machining of SiC ceramic matrix composites: a review[J]. Chinese J Aeronaut 34(4):540–567
9. Cao JG, Wu YB, Lu D, Fujimoto M, Nomura M (2014) Fundamental machining characteristics of ultrasonic assisted internal grinding of SiC ceramics[J]. Mater Manuf Process 29(5):557–563
10. Prasad BS, Babu MP (2017) Correlation between vibration amplitude and tool wear in turning: numerical and experimental analysis[J]. Eng Sci Technol 20(1):197–211
11. Shen JY, Wang JQ, Jiang B, Xu XP (2015) Study on wear of diamond wheel in ultrasonic vibration-assisted grinding ceramic[J]. Wear 332:788–793
12. Palanikumar K, Davim JP (2007) Mathematical model to predict tool wear on the machining of glass fibre reinforced plastic composites[J]. Mater Design 28(7):2008–2014
13. Das D, Chakraborty V (2018) Dry condition machining performance of T6 treated aluminium matrix composites[J]. Mater Today: Proc 5(9):20145–20151
14. Airao J, Nirala CK, Lacalle LNL, Khanna N (2021) Tool wear analysis during ultrasonic assisted turning of nimonic-90 under dry and wet conditions[J]. Metals 11(8):1253
15. Feng YX, Hsu FC, Lu YT, Lin CT, Lin CF, Lu YC, Liang SY (2020) Tool wear rate prediction in ultrasonic vibration-assisted milling[J]. Mach Sci Technol 24(5):758–780
16. Liu HZ, Zong WJ (2019) Prediction model of tool wear volume in precision turning of ceramic particle reinforced aluminum matrix composites[J]. Int J Adv Manuf Technol 100(9):2689–2700
17. Ma LJ, Sun ZC, Zhang L, Deng H, Tan YQ, Kong Z, Wei ZQ (2020) Study on mechanism and theoretical model of tool wear in fluorophlogopite glass-ceramics turning[J]. J Mater Process Technol 275:116284
18. Zhao H, Zhou M (2008) An experimental study on diamond cutting of optical glass[C]//Key Engineering Materials. Trans Tech Publications Ltd 375:211–215
19. Sarma DK, Dixit US (2007) A comparison of dry and air-cooled turning of grey cast iron with mixed oxide ceramic tool[J]. J Mater Process Technol 190(1–3):160–172
20. Dai CW, Yin Z, Wang P, Miao Q, Chen JJ (2021) Analysis on ground surface in ultrasonic face grinding of silicon carbide (SiC) ceramic with minor vibration amplitude[J]. Ceram Int 47(15):21959–21968
21. Rajasekaran T, Palanikumar K, Vinayagam BK (2012) Turning CFRP composites with ceramic tool for surface roughness analysis[J]. Procedia Eng 38:2922–2929
22. Shan CW, Wang X, Yang XX, Lyu XB (2016) Prediction of cutting forces in ball-end milling of 25 D C/C composites[J]. Chinese J Aeronaut 29(3):824–830
23. Babbar A, Sharma A, Jain V, Jain AK (2019) Rotary ultrasonic milling of C/SiC composites fabricated using chemical vapor infiltration and needling technique[J]. Mater Res Express 6(8):085607
24. Zhang B, Du YN, Liu HL, Xin LJ, Yang YF, Liang Li (2021) Experimental study on high-speed milling of SiC$_f$/SiC composites with PCD and CVD diamond tools[J]. Materials 14(13):3470
25. Dhokey NB, Utpat K, Gosavi A, Dhoka P (2013) Hot-press sintering temperature response of diamond cutting tools and its correlation with wear mechanism[J]. Int J Refract Met Hard Mater 36:289–293
26. Kılıckap E, Cakır O, Aksoy M, İnan A (2005) Study of tool wear and surface roughness in machining of homogenised SiC-p reinforced aluminium metal matrix composite[J]. J Mater Process Technol 164:862–867
27. Bhushan RK (2020) Impact of nose radius and machining parameters on surface roughness, tool wear and tool life during turning of AA7075/SiC composites for green manufacturing[J]. Mech Adv Mater Mod Process 6(1):1–18
28. Wu X, Li L, He N, Zhao GL, Jiang F, Shen JY (2018) Study on the tool wear and its effect of PCD tool in micro milling of tungsten carbide[J]. Int J Refract Met Hard Mater 77:61–67
29. Li X, Seah WKH (2001) Tool wear acceleration in relation to workpiece reinforcement percentage in cutting of metal matrix composites[J]. Wear 247(2):161–171

30. Quan YM, Zhou ZH (2000) Tool wear and its mechanism for cutting SiC particle-reinforced aluminium matrix composites[J]. J Mater Process Technol 100(1–3):194–199

31. Zeng WM, Li ZC, Pei ZJ, Treadwell (2005) Experimental observation of tool wear in rotary ultrasonic machining of advanced ceramics[J]. Int J Mach Tool Manu 45(12–13):1468–1473

32. Liu Y, Liu ZB, Wang XB, Huang T (2020) Experimental study on tool wear in ultrasonic vibration–assisted milling of C/SiC composites[J]. Int J Adv Manuf Technol 107(1):425–436

33. Wang H, Hu YB, Cong WL, Hu ZL (2019) A mechanistic model on feeding-directional cutting force in surface grinding of CFRP composites using rotary ultrasonic machining with horizontal ultrasonic vibration[J]. Int J Mech Sci 155:450–460

34. Wang JJ, Feng PF, Zhang JF, Guo P (2018) Reducing cutting force in rotary ultrasonic drilling of ceramic matrix composites with longitudinal-torsional coupled vibration[J]. Manuf Lett 18:1–5

35. Wang JJ, Zhang JF, Feng PF, Guo P, Zhang QL (2018) Feasibility study of longitudinal–torsional-coupled rotary ultrasonic machining of brittle material[J]. J Manuf Sci Eng 140(5):051008

36. Tool-Life Testing with Single-Point Turning Tools (1993) International standards, ISO 3685–1993(E). International Organization for Standardization, Geneva

37. Ning F, Cong W (2020) Ultrasonic vibration-assisted (UV-A) manufacturing processes: State of the art and future perspectives[J]. J Manuf Process 51:174–190

38. Peng ZL, Zhang XY, Zhang DY (2021) Effect of radial high-speed ultrasonic vibration cutting on machining performance during finish turning of hardened steel[J]. Ultrasonics 111:106340

39. Júnior MG, França TV, Fortulan CA, Silva RHLD, Foschini CR (2022) Green ceramic machining benefits through ultrasonic-assisted turning: an experimental investigation[J]. Int J Adv Manuf Technol 118(9):3091–3104

40. Xiong YF, Wang W, Jiang R, Liu C (2022) Feasibility and tool performance of ultrasonic vibration-assisted milling-grinding SiC_f/SiC ceramic matrix composite[J]. J Mater Res Technol 19:3018–3033

Publisher's Note Springer Nature remains neutral with regard to jurisdictional claims in published maps and institutional affiliations.

Springer Nature or its licensor (e.g. a society or other partner) holds exclusive rights to this article under a publishing agreement with the author(s) or other rightsholder(s); author self-archiving of the accepted manuscript version of this article is solely governed by the terms of such publishing agreement and applicable law.